

Article

Spatial and Temporal Variability of Soil Respiration between Soybean Crop Rows as Measured Continuously over a Growing Season

Xiaohan Wang ¹ and Tusheng Ren ^{2,*}

¹ School of Geographic and Oceanographic Sciences, Nanjing University, Nanjing 210023, China; wangxiaohan0203@163.com

² Department of Soil and Water Science, China Agricultural University, Beijing 100193, China

* Correspondence: tsren@cau.edu.cn

Academic Editors: Federica De Leo, Pier Paolo Miglietta and Marc A. Rosen

Received: 25 December 2016; Accepted: 14 March 2017; Published: 16 March 2017

Abstract: An improved understanding of temporal and spatial variations in soil respiration is essential for measuring soil CO₂ effluxes accurately. In this study, a field experiment was conducted to investigate the spatial and temporal variability of soil respiration between adjacent crop rows in a soybean (*Glycine max* L.) field. Soil CO₂ concentration, water content, and temperature at a 7.5 cm depth were recorded continuously at 0 cm, 12 cm, 24 cm, and 35 cm from the plant row during the growing season. Root biomass at the corresponding locations was collected from the 0 to 10 cm and 10 to 20 cm soil layers at three growth stages. Seasonal CO₂ efflux data showed that the minimum value appeared at the seeding stage, increased gradually, reached the maximum at the flowering and grain-filling stages, and then dropped steadily at the mature stage. Within a growth stage, CO₂ effluxes related positively to soil temperature, but negatively to soil water content. In the early and vigorous growing stages of soybean crop, soil respiration showed apparent diurnal variations, and was most significant at the crop row location. Except for the seeding stage, CO₂ effluxes at the crop row were larger than that of other locations, and effluxes at 35 cm from the row were representative of the mean CO₂ efflux between adjacent rows. We concluded that the spatial heterogeneity of CO₂ efflux between crop rows should be taken into consideration when measuring soil respiration in agricultural ecosystems.

Keywords: soil CO₂ efflux; spatial and temporal variability; *Glycine max* L.; crop growth stages

1. Introduction

Soil respiration, the second largest carbon flux in agricultural ecosystems [1], involves the generation and transport of CO₂ produced by biochemical processes, including root activities and soil organisms' metabolism [2–5]. Numerous studies have shown that the spatial-temporal variation in soil CO₂ effluxes is significant at different scales and is sensitive to environmental factors, such as soil temperature [6,7], soil water [8,9], soil texture [10,11], and root density [12]. Limited information about differentiation and diversities at various scales brings about measurement uncertainties of CO₂ efflux from soil [13–15]. There is evidence that soil properties (e.g., total biomass and soil nitrogen levels) affect soil respiration differently from cm to km levels [16,17].

Accurate estimation of soil respiration at field and crop row scales is essential for assessing ecosystem carbon budget. However, few studies have focused on the spatial variation in soil respiration at micro-scales, e.g., between and within crop rows. Previous work has shown that soil temperature, soil water content, and root biomass distribute non-uniformly between crop rows [18–20], which may affect the spatial and temporal distribution of soil respiration, and consequently CO₂ efflux at the

row scale. In many field studies, however, CO₂ measurement positions are chosen randomly [21–23], which fails to account for the spatial variability of soil respiration between crop rows.

The objective of this study was to investigate the spatial and temporal variability of soil respiration between adjacent crop rows and the relevant soil CO₂ emission at the field scale.

2. Materials and Methods

2.1. Site Description

The study was conducted in a soybean field at the Lishu Experimental Station of China Agricultural University, located in Jilin Province, China (124°22'E, 43°10'N). The region has a temperate semi-humid monsoon climate with mean annual precipitation of 573 mm and a mean annual air temperature of 5.9 °C [24]. The soil texture was silty clay loam (16.7% sand, 45.8% silt, and 37.5% clay) according to the USDA classification system [25]. Soybean (*Glycine max* L.) was sown on Day Of Year (DOY) 132 and harvested on DOY 278 of 2013, at a row spacing of 70 cm. A compound fertilizer (N/P/K = 15:15:15) was applied in the crop row at a rate of 500 kg·ha⁻¹ at the planting time.

2.2. Soil and CO₂ Concentration Measurements

Soil CO₂ concentration was monitored continuously from DOY 152 to DOY 274 with CO₂ probes (model GMT221, Vaisala Inc., Helsinki, Finland). The cylindrical probes are 155 mm long and 18.5 mm in diameter. In order to characterize the soil respiration rate at various distances from the plant row, four probes were placed at 0, 12, 24, and 35 cm away from the plant row and at the depth of 7.5 cm (Figure 1). Four soil temperature sensors (50 cm long and 4 mm in diameter, AV-10T-H, Avalon, USA) were also installed at the corresponding locations. The CO₂ and temperature sensors were connected to a data logger (RR-1010, Yugen Scientific, Inc., Beijing, China) that recorded the measurements every 30 min and reported the mean values every hour. In addition, soil water content at the 4 locations was recorded with a TDR 100 system (Campbell Scientific, Inc., Logan, UT, USA). The length, rod diameter, and rod-to-rod spacing of the TDR probes are 150 mm, 4.8 mm, and 22.5 mm, respectively.

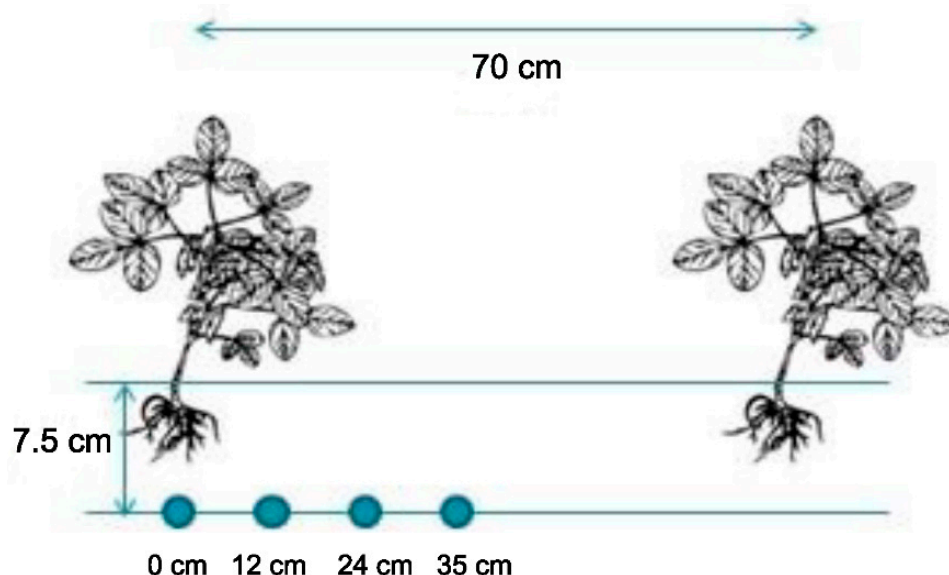


Figure 1. Schematic view of the CO₂ monitoring locations between adjacent two crop rows.

Plant root density was measured at the flower bud differentiation stage, at the flowering and grain-filling stages, and at the mature stage. Soil samples were excavated with a root auger (10 cm in diameter) from the 0–10 cm and 10–20 cm soil layers at 0, 12, 24, and 35 cm away from the plant row.

The measurements were replicated three times. After washing soil particles, fresh roots were collected and oven-dried at 80 °C to a constant mass, and root biomass density was estimated.

2.3. Estimation of Soil CO₂ Concentration and Data Analysis

The CO₂ concentration collected with the data logger was expressed in volume fraction (ppm), which was converted to mole concentration ($\mu\text{mol}\cdot\text{m}^{-3}$) [26]. We estimated CO₂ flux at the soil surface by assuming that CO₂ concentration at the soil surface was 380 ppm [27], and CO₂ diffused away one dimensionally from the soil. Thus, CO₂ flux was estimated by using the Fick's first law of gas diffusion [26],

$$F = -D_s \frac{dC}{dz} \quad (1)$$

where F is CO₂ efflux ($\mu\text{mol}\cdot\text{m}^{-2}\cdot\text{s}^{-1}$), D_s is CO₂ diffusivity in soil ($\text{m}^2\cdot\text{s}^{-1}$), and $\frac{dC}{dz}$ ($\mu\text{mol}\cdot\text{m}^{-3}$) is the vertical CO₂ concentration gradient from soil surface to depth z (0.075 m).

Parameter D_s was computed according to the Millington–Quirk model [28],

$$D_s = D_0 \times \frac{\varepsilon^{\frac{10}{3}}}{\varphi^2} \quad (2)$$

where D_0 is the CO₂ diffusion coefficient in free air, ε is volumetric air content (air-filled porosity), and φ is the soil porosity.

D_0 is a function of temperature and was calculated using the Armstrong model [29],

$$\log_{10} D_0 = 1.9975 \times \log_{10}(T + 273.15) - 9.7273 \quad (3)$$

where T is soil temperature (K).

Soil porosity φ is the sum of ε and the volumetric water content (θ), which was estimated using the following equation:

$$\varphi = 1 - \frac{\rho_b}{\rho_s} = \varepsilon + \theta \quad (4)$$

where ρ_b and ρ_s are soil the bulk density and particle density, respectively. The soil particle density ρ_s was assumed to be $2.65 \text{ g}\cdot\text{cm}^{-3}$ [30].

For soil bulk density determination, three soil cores were collected before soybean seeding with a ring sampler and oven-dried at 105 °C in laboratory. The average value was $1.42 \text{ g}\cdot\text{cm}^{-3}$.

Linear correlation analysis was conducted to determine the relationships between CO₂ efflux and soil temperature and water content. Differences of root biomass density among the four measurement locations were tested statistically. Data analyses were performed by using the SPSS 11.0 package (SPSS, Chicago, IL, USA).

3. Results and Discussion

3.1. Seasonal Variation in Soil CO₂ Efflux

Figure 2 presents the seasonal variation in soil CO₂ efflux, soil temperature, and soil water content at 0, 12, 24, and 35 cm from DOY 153 to DOY 274. There are some missing data due to equipment malfunction. The CO₂ effluxes were lower at crop emergence and vegetative growing stages (before DOY 171), then increased gradually with time and reached the maximum at the flowering and grain-filling stages (from DOY 171 to DOY 240), and dropped steadily at the mature stage (after DOY 240). The maximum CO₂ efflux, $1.84 \mu\text{mol}\cdot\text{m}^{-2}\cdot\text{s}^{-1}$, appeared on DOY 239. Except for the seeding stage, the CO₂ efflux at the crop row (i.e., at 0 cm) was larger than that of other locations. For all four locations, the mean CO₂ effluxes were lowest at the seeding stage (Figure 2).

Soil water content and soil temperature are the two main factors controlling soil respiration rate [11,31]. Within a growth stage, soil respiration related positively to soil temperature except for

the 24 cm location at the seeding stage and the 0 cm location at the flowering and grain-filling stages (Table 1), while soil water content related negatively to the soil respiration rate (Table 2). Our results agreed with Xu and Qi [15] who found that the seasonal trend of the soil CO₂ efflux followed that of the soil temperature rather than the soil moisture when soil water content was relatively high. Frequent precipitation since June (i.e., about 47.8 mm more than that of the normal years) led to a high level of soil water content that ranged from 0.25 to 0.50 m³·m⁻³. As a result, soil respiration and CO₂ flow was restricted due to the limited availability of oxygen [32,33] and the reduced diffusion pathways [21].

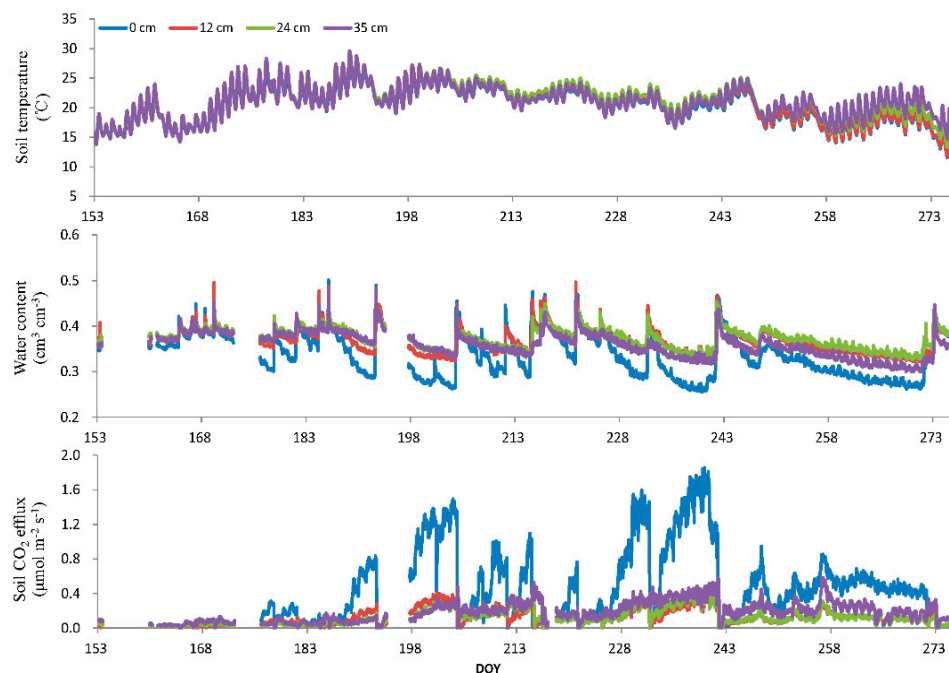


Figure 2. Seasonal variations in soil water content, temperature, and soil CO₂ efflux at 0, 12, 24, and 35 cm from the plant row.

The increase in soil CO₂ efflux with temperature at the early stages (until the flowering and grain-filling stages) was caused in part by the promotion effect of temperature on root biomass production [34,35]. Root respiration is a major component of soil respiration, and the contribution of root respiration to the soil CO₂ efflux can be very high: 50%–93% in arctic tundra [36], 35%–62% in boreal forests [37], and as high as 60% in farmlands [38]. Plant root respiration and root density usually reach the maximum at about the same time [39].

Table 1. Pearson correlation coefficients between soil temperature and soil CO₂ efflux at the four observation locations for the four crop growth stages.

Crop Growth Stage	Coefficients of Correlation			
	0 cm	12 cm	24 cm	35 cm
Seeding stage	0.23 **	0.28 **	0.09	0.19 **
Flower bud differentiation stage	0.68 **	0.54 **	0.37 **	0.18 **
Flowering and grain-filling stages	−0.16 **	0.60 **	0.37 **	0.36 **
Mature stage	0.14 **	0.09	0.10 **	0.59 **

Means followed by the stars (**) indicate significant correlation between soil temperature and soil CO₂ efflux ($p < 0.01$).

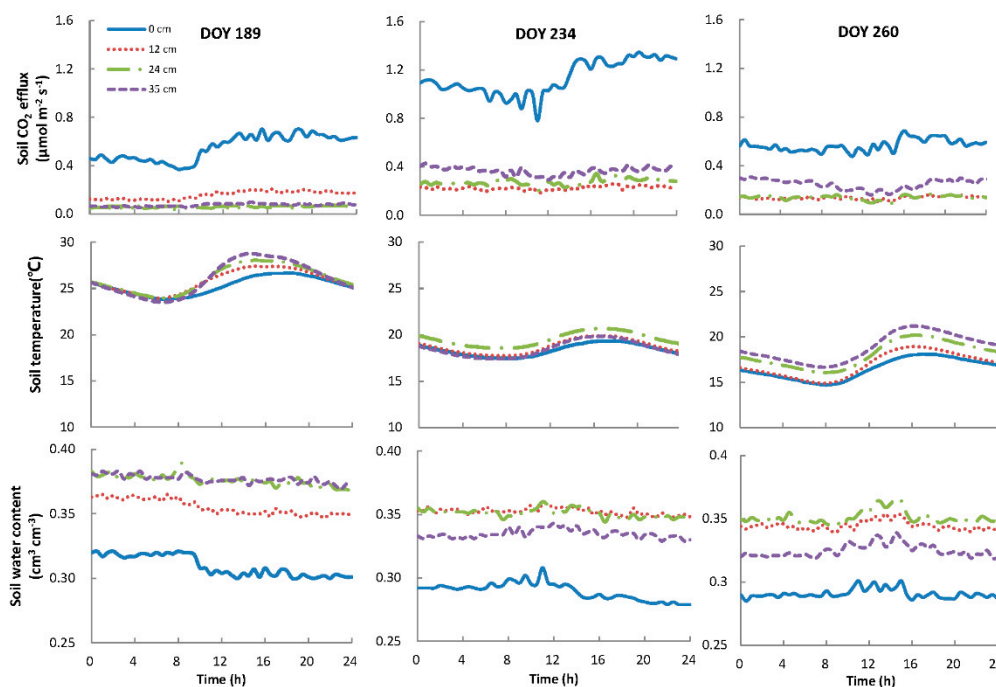
Table 2. Pearson correlation coefficients between soil water content and soil CO₂ efflux at the four observation locations for the four crop growth stages.

Crop Growth Stage	Coefficients of Correlation			
	0 cm	12 cm	24 cm	35 cm
Seeding stage	−0.71 **	−0.83 **	−0.94 **	−0.69 **
Flower bud differentiation stage	−0.76 **	−0.76 **	−0.94 **	−0.57 **
Flowering and grain-filling stages	−0.65 **	−0.68 **	−0.92 **	−0.54 **
Mature stage	−0.53 **	−0.57 **	−0.82 **	−0.31 **

Means followed by the stars (**) indicate significant correlation between soil moisture and soil CO₂ efflux ($p < 0.01$).

3.2. Diurnal Variation in Soil CO₂ Efflux

We selected three sunny days, DOY 189, DOY 234, and DOY 260, which represented the flower bud differentiation stage, the flowering and grain-filling stages, and the mature stage, respectively, to demonstrate the daily variations in soil CO₂ efflux, soil temperature, and water content (Figure 3). While there were strong diurnal soil temperature variations in all cases, no apparent diurnal soil water content changes were observed. The CO₂ efflux responded dynamically to soil temperature: it was at the minimum at 5:00–8:00, increased gradually and reached the maximum at 15:00–18:00, and then decreased slowly. The trend was especially clear in the early and vigorous growing stages of the root zone (i.e., the 0 cm location). In addition, the CO₂ efflux at the flowering and grain-filling stages (the peak growing season with the highest temperature) was significantly higher than that of the other periods. Thus, the diurnal CO₂ efflux fluctuation was driven primarily by soil temperature changes. This is explained by the fact that root (autotrophic) and microbial (heterotrophic) activities are increased with temperature [40].

**Figure 3.** Daily variations in soil water content, temperature, and soil CO₂ efflux at 0, 12, 24, and 35 cm from the plant.

It was interesting to observe that the CO₂ efflux generally lagged behind soil temperature during the early growing seasons, but was in pace with soil temperature in the late growing stages (Figure 3), which agreed with the report of Parkin and Kaspar [41] who observed a phase shift between soil CO₂

efflux and soil temperature. Riveros-Iregui et al. [42] demonstrated that diurnal hysteresis between soil CO₂ and soil temperature was controlled mainly by soil water content. Comparing with conditions at low water content levels, a larger amount of soil water resulted in a greater CO₂ production rate but a lower CO₂ diffusion rate [42].

Correlation analysis showed that there was a significant negative correlation between CO₂ efflux and soil water content, an indication that high water content might have limited CO₂ production and transport. There was a positive correlation between soil respiration and soil temperature in the row, especially at the early growing seasons, but the correlation became smaller with distance from crop row, and eventually disappeared at 24 and 35 cm away from the crop, especially at the mature stage (Table 3).

Table 3. Correlation coefficients between diurnal soil CO₂ efflux and soil water content and soil temperature at 0, 12, 24, and 35 cm away from the plant row in the soybean field.

Distance to Plant Row	Soil Temperature				Soil Water Content			
	0 cm	12 cm	24 cm	35 cm	0 cm	12 cm	24 cm	35 cm
DOY 175	0.87 **	0.90 **	0.65 **	0.77 **	−0.96 **	−0.97 **	−0.97 **	−0.88 **
DOY 219	0.73 **	0.41 **	0.32 **	−0.05	−0.98 **	−0.93 **	−0.97 **	−0.96 **
DOY 249	0.71 **	0.24	−0.02	−0.23	−0.63 **	−0.80 **	−0.92 **	−0.94 **

Means followed by the stars (**) indicate significant correlation between diurnal soil CO₂ efflux and soil temperature and soil water content ($p < 0.01$).

3.3. Spatial Heterogeneity of the Soil CO₂ Efflux

A strong inter-row spatial variability of CO₂ efflux was observed in both seasonal and diurnal results, and the variability differed among the crop growth stages (Figures 2 and 3). At the seeding stage, the magnitude of CO₂ efflux was in the order of 35 cm > 24 cm > 12 cm > 0 cm, which followed the spatial pattern of soil water content distribution. In the bud differentiation period and pod formation stages, CO₂ efflux was higher in the crop row (0 cm) than that of other positions, which might be caused by the greater root biomass and therefore higher root respiration rates in the crop row (Table 4). At the pod-filling and grain maturity stages, the CO₂ efflux followed the order of 0 cm > 35 cm > 24 cm > 12 cm. The highest root biomass and the lowest water content level produced the highest CO₂ efflux in the crop row. For the other locations, the magnitude of the CO₂ efflux was a result of the joint effect of plant respiration and water content. Soil water content was the dominant factor related to the CO₂ efflux. At the 12 cm location, low air-filled porosity limited CO₂ transfer in soil and resulted in a lower CO₂ efflux. On the other hand, higher air-filled porosity at the 35 cm location produced a higher CO₂ efflux than that of the 12 cm location, although the root biomass at 35 cm was relatively lower. The spatial pattern of soil temperature among the four locations during the growing season was not clear, which explained why temperature did not drive differences in the CO₂ efflux among the locations.

Table 4. Root biomass density (g·cm^{−3}) determined at 0, 12, 24, and 35 cm away from the plant row in the 0–10 cm and 10–20 cm soil layers.

Distance To Plant Row	0–10 cm Soil Layer				10–20 cm Soil Layer			
	0 cm	12 cm	24 cm	35 cm	0 cm	12 cm	24 cm	35 cm
DOY 175	1128.96 **	65.35	29.34	11.68	20.93	23.99	13.16	13.89
DOY 219	2904.88 **	316.31	117.32	102.55	204.2	136.14	118.47	30.32
DOY 249	6492.44 **	159.28	123.31	69.28	115.58 *	58.43	34.44	27.64

Means followed by the star (*) in a row differed significantly at $p < 0.05$.

The spatial heterogeneity of the soil CO₂ efflux was also reflected in the daily variation in soil respiration. The daily ranges of CO₂ efflux at the 0, 12, 24, and 35 cm locations were 0.40, 0.06, 0.10,

and $0.06 \mu\text{mol}\cdot\text{m}^{-2}\cdot\text{s}^{-1}$, respectively (Figure 3). The daily amplitude of the CO_2 efflux in the row was significantly higher than that of other positions because root biomass at this location was the highest, which boosted soil respiration [43,44]. Over the entire growing season, the average soil CO_2 efflux at locations 0, 12, 24, and 35 cm away from the plant row were 0.444, 0.126, 0.126, and $0.187 \mu\text{mol}\cdot\text{m}^{-2}\cdot\text{s}^{-1}$, respectively, and the synthetic average soil CO_2 efflux of all positions was $0.221 \mu\text{mol}\cdot\text{m}^{-2}\cdot\text{s}^{-1}$. Thus, for this study, the soil CO_2 efflux at 35 cm away from the plants approached the average of the CO_2 effluxes of the four locations during the soybean growth period.

Many researchers have shown that soil respiration is characterized by high spatial and temporal variations among different ecosystems [22,45,46]. Soil temperature and water, which are the key environmental factors controlling CO_2 effluxes from soil, also affect root biomass and its activity [47]. Systematic spatial patterns of soil temperature and water content [48] control the spatial heterogeneity of soil respiration and CO_2 effluxes. Higher soil respiration occurs generally near the plant as a result of greater root biomass than locations away from the plant [13,34,49–51]. In our research, the CO_2 efflux at the 0 cm position was higher than that at other locations, which was consistent with previous findings. The seasonal variation in soil respiration was mainly due to temporal patterns of temperature and plant growth, while the radial gradient in total root biomass and the spatial distribution of water content were the dominant factors of inter-row spatial heterogeneity of the soil CO_2 effluxes among the four locations.

It is difficult to estimate soil respiration due to its high spatial variability [13,14]. The complex spatial patterns of soil properties (e.g., soil temperature, water, and root biomass) enhance the spatial variability of soil CO_2 efflux. For more accurate measurements and calculations of soil CO_2 effluxes in agricultural ecosystems, the arrangement of observation locations should be considered carefully [52]. For this particular study, it appears that the average CO_2 efflux at 35 cm from the crop row was representative of the mean CO_2 efflux between any two crop rows.

4. Conclusions

We investigated the spatial and temporal variability of soil CO_2 effluxes within crop rows in a soybean field by in situ monitoring soil CO_2 effluxes during the growing season. The CO_2 efflux was low during early growth stages and reached the maximum at the flowering and grain-filling stages. The diurnal soil CO_2 efflux generally lagged behind soil temperature. Soil temperature was the key factor that drove the seasonal and diurnal variability of CO_2 efflux. A strong inter-row spatial variability of CO_2 efflux was observed in both seasonal and diurnal results: the soil CO_2 efflux under the plants was significant larger than that of other locations between crop rows, due to the higher root biomass. The spatial and temporal heterogeneity of soil respiration should be considered for more accurate measurement and estimation of soil respiration rate.

Acknowledgments: This research was funded by the Basic Research Development Program of China (No. 2015CB150403).

Author Contributions: Tusheng Ren and Xiaohan Wang designed the research and wrote the paper jointly. Xiaohan Wang conducted field experiments and analyzed the data.

Conflicts of Interest: The authors declare no conflict of interest.

References

1. Wan, S.; Norby, R.J.; Ledford, J.; Weltzin, J.F. Responses of soil respiration to elevated CO_2 , air warming, and changing soil water availability in a model old-field grassland. *Glob. Chang. Biol.* **2007**, *13*, 2411–2424. [[CrossRef](#)]
2. Lundegårdh, H. Carbon dioxide evolution and crop growth. *Soil Sci.* **1927**, *23*, 417–453. [[CrossRef](#)]
3. Fang, C.; Moncrieff, J.B. A model for soil CO_2 production and transport: 1. Model development. *Agric. For. Meteorol.* **1999**, *95*, 225–236. [[CrossRef](#)]
4. Hanson, P.J.; Edwards, N.T.; Garten, C.T.; Andrews, J.A. Separating root and soil microbial contributions to soil respiration: A review of methods and observations. *Biogeochemistry* **2000**, *48*, 115–146. [[CrossRef](#)]

5. Saiz, G.; Black, K.; Reidy, B.; Lopez, S.; Farrell, E.P. Assessment of soil CO₂ efflux and its components using a process-based model in a young temperate forest site. *Geoderma* **2007**, *139*, 79–89. [[CrossRef](#)]
6. Ross, D.J.; Cairns, A. Influence of temperature on biochemical processes in some soils from tussock grasslands. *N. Z. J. Sci.* **1978**, *21*, 581–589.
7. Howard, P.J.A.; Howard, D.M. Respiration of decomposing litter in relation to temperature and moisture: Microbial decomposition of tree and shrub leaf litter 2. *Oikos* **1979**, *33*, 457–465. [[CrossRef](#)]
8. Rixon, A.J. Oxygen uptake and nitrification at various moisture levels by soils and mats from irrigated pastures. *J. Soil Sci.* **1968**, *19*, 56–66. [[CrossRef](#)]
9. Rixon, A.J.; Bridge, B.J. Respiratory quotient arising from microbial activity in relation to matric suction and air filled pore space of soil. *Nature* **1968**, *218*, 961–962. [[CrossRef](#)] [[PubMed](#)]
10. Hanson, P.J.; Wullschlegel, S.D.; Bohlman, S.A.; Todd, D.E. Seasonal and topographic patterns of forest floor CO₂ efflux from an upland oak forest. *Tree Physiol.* **1993**, *13*, 1–15. [[CrossRef](#)] [[PubMed](#)]
11. Davidson, E.A.; Belk, E.; Boone, R.D. Soil water content and temperature as independent or confounded factors controlling soil respiration in a temperate mixed hardwood forest. *Glob. Chang. Biol.* **1998**, *4*, 217–227. [[CrossRef](#)]
12. Janssens, I.A.; Crookshanks, M.; Taylor, G.; Ceulemans, R. Elevated atmospheric CO₂ increases fine root production, respiration, rhizosphere respiration and soil CO₂ efflux in scots pine seedlings. *Glob. Chang. Biol.* **2002**, *4*, 871–878. [[CrossRef](#)]
13. Fang, C.; Moncrieff, J.B.; Gholz, H.L.; Clark, K.L. Soil CO₂ efflux and its spatial variation in a florida slash pine plantation. *Plant Soil* **1998**, *205*, 135–146. [[CrossRef](#)]
14. Stoyan, H.; De-Polli, H.; Böhm, S.; Robertson, G.P.; Paul, E.A. Spatial heterogeneity of soil respiration and related properties at the plant scale. *Plant Soil* **2000**, *222*, 203–214. [[CrossRef](#)]
15. Xu, M.; Qi, Y. Soil-surface CO₂ efflux and its spatial and temporal variations in a young ponderosa pine plantation in Northern California. *Glob. Chang. Biol.* **2001**, *7*, 667–677. [[CrossRef](#)]
16. Poberston, G.P.; Gross, K.L. *Assessing the Heterogeneity of Belowground Resources: Quantifying Pattern and Scale*; Academic Press: New York, NY, USA, 1994.
17. Franklin, R.B.; Mills, A.L. Multi-scale variation in spatial heterogeneity for microbial community structure in an Eastern Virginia agricultural field. *FEMS Microbiol. Ecol.* **2003**, *44*, 335–346. [[CrossRef](#)]
18. Lemon, E.R.; Wiegand, C.L. Soil aeration and plant root relations II. Root respiration. *Agron. J.* **1962**, *54*, 171–175. [[CrossRef](#)]
19. Tardieu, F. Analysis of the spatial variability of maize root density. *Plant Soil* **1988**, *107*, 259–266. [[CrossRef](#)]
20. Van Wesenbeeck, I.J.; Kachanoski, R.G. Spatial and temporal distribution of soil water in the tilled layer under a corn crop. *Soil Sci. Soc. Am. J.* **1988**, *52*, 363–368. [[CrossRef](#)]
21. Rochette, P.; Desjardins, R.L.; Pattey, E. Spatial and temporal variability of soil respiration in agricultural fields. *Can. J. Soil Sci.* **1991**, *71*, 189–196. [[CrossRef](#)]
22. Buyanovsky, G.A.; Wagner, G.H.; Gantzer, C.J. Soil respiration in a winter wheat ecosystem. *Soil Sci. Soc. Am. J.* **1986**, *50*, 338–344. [[CrossRef](#)]
23. Lai, L.; Zhao, X.; Jiang, L.; Wang, Y.; Luo, L.; Zheng, Y.; Chen, X.; Rimmington, G.M. Soil respiration in different agricultural and natural ecosystems in an arid region. *PLoS ONE* **2012**, *7*, e48011. [[CrossRef](#)] [[PubMed](#)]
24. Zhang, B.; Li, Y.; Ren, T.; Tian, Z.; Wang, G.; He, X.; Tian, C. Short-term effect of tillage and crop rotation on microbial community structure and enzyme activities of a clay loam soil. *Biol. Fertil. Soils* **2014**, *50*, 1077–1085. [[CrossRef](#)]
25. Gee, G.W.; Or, D. *Particle-Size Analysis*; Soil Science Society of America: Madison, WI, USA, 2002.
26. Tang, J.; Baldocchi, D.D.; Qi, Y.; Xu, L. Assessing soil CO₂ efflux using continuous measurements of CO₂ profiles in soils with small solid-state sensors. *Agric. For. Meteorol.* **2003**, *118*, 207–220. [[CrossRef](#)]
27. Intergovernmental Panel on Climate Change (IPCC). *Climate Change 2007: Impacts, Adaptation and Vulnerability*; Working Group II Contribution to the Fourth Assessment Report of the Intergovernmental Panel on Climate Change; Cambridge University Press: Cambridge, UK, 2007.
28. Millington, R.J.; Quirk, J.P. Permeability of porous solids. *Trans. Faraday Soc.* **1961**, *57*, 1200–1207. [[CrossRef](#)]
29. Armstrong, W. Aeration in higher plants. *Adv. Bot. Res.* **1979**, *7*, 225–332.
30. Schjønning, P.; McBride, R.A.; Keller, T.; Obour, P.B. Predicting soil particle density from clay and soil organic matter contents. *Geoderma* **2017**, *286*, 83–87. [[CrossRef](#)]

31. Janssens, I.A.; Lankreijer, H.; Matteucci, G.; Kowalski, A.S.; Buchmann, N.; Epron, D.; Pilegaard, K.; Kutsch, W.; Longdoz, B.; Grünwald, T.; et al. Productivity overshadows temperature in determining soil and ecosystem respiration across European forests. *Glob. Chang. Biol.* **2002**, *7*, 269–278. [[CrossRef](#)]
32. Linn, D.M.; Doran, J.W. Effect of water-filled pore space on carbon dioxide and nitrous oxide production in tilled and nontilled soils. *Soil Sci. Soc. Am. J.* **1984**, *48*, 1267–1272. [[CrossRef](#)]
33. Skopp, J.; Jawson, M.D.; Doran, J.W. Steady-state aerobic microbial activity as a function of soil water content. *Soil Sci. Soc. Am. J.* **1990**, *54*, 1619–1625. [[CrossRef](#)]
34. Wiseman, P.E.; Seiler, J.R. Soil CO₂ efflux across four age classes of plantation loblolly pine (*Pinus taeda* L.) on the virginia piedmont. *For. Ecol. Manag.* **2004**, *192*, 297–311. [[CrossRef](#)]
35. Boone, R.D.; Nadelhoffer, K.J.; Canary, J.D.; Kaye, J.P. Roots exert a strong influence on the temperature sensitivity of soil respiration. *Nature* **1998**, *396*, 570–572. [[CrossRef](#)]
36. Billings, W.D.; Peterson, K.M.; Shaver, G.R.; Trent, A.W. Root growth, respiration, and carbon dioxide evolution in an arctic tundra soil. *Arct. Alp. Res.* **1977**, *9*, 129–137. [[CrossRef](#)]
37. Ryan, M.G.; Lavigne, M.G.; Gower, S.T. Annual carbon cost of autotrophic respiration in boreal forest ecosystems in relation to species and climate. *J. Geophys. Res.* **1997**, *102*, 28871–28883. [[CrossRef](#)]
38. Rochette, P.; Flanagan, L.B. Quantifying rhizosphere respiration in a corn crop under field conditions. *Soil Sci. Soc. Am. J.* **1996**, *61*, 466–474. [[CrossRef](#)]
39. Schüller, W.; Neubert, R.; Levin, I.; Fischer, N.; Sonntag, C. Determination of microbial versus root produced CO₂ in an agricultural ecosystem by means of $\delta^{13}\text{CO}_2$ measurements in soil air. *Tellus Ser. B Chem. Phys. Meteorol.* **2000**, *52*, 909–918. [[CrossRef](#)]
40. Zogg, G.; Zak, D.R.; Burton, A.; Pregitzer, K. Fineroot respiration in northern hardwood forests in relation to temperature and nitrogen availability. *Tree Physiol.* **1996**, *16*, 719–725. [[CrossRef](#)] [[PubMed](#)]
41. Parkin, T.B.; Kaspar, T. Temperature controls on diurnal carbon dioxide flux implications for estimating soil carbon loss. *Soil Sci. Soc. Am. J.* **2003**, *67*, 1763–1772. [[CrossRef](#)]
42. Riveros-Iregui, D.; Emanuel, R.; Muth, D.J.; Wraith, J.M. Hysteresis between soil temperature and soil CO₂ is controlled by soil water content. *Geophys. Res. Lett.* **2007**, *34*, 138. [[CrossRef](#)]
43. Bouma, T.J.; Bryla, D.R. On the assessment of root and soil respiration for soils of different textures: Interactions with soil moisture contents and soil CO₂ concentrations. *Plant Soil* **2000**, *227*, 215–221. [[CrossRef](#)]
44. Kuzyakov, Y.; Cheng, W. Photosynthesis controls of rhizosphere respiration and organic matter decomposition. *Soil Biol. Biochem.* **2001**, *33*, 1915–1925. [[CrossRef](#)]
45. Toland, D.E.; Zak, D.R. Seasonal patterns of soil respiration in intact and clear-cut northern hardwood forests. *Can. J. For. Res.* **1994**, *24*, 1711–1716. [[CrossRef](#)]
46. Paustian, K.; Elliott, E.T.; Peterson, G.A.; Killian, K. Modelling climate, CO₂ and management impacts on soil carbon in semi-arid agroecosystems. *Plant Soil* **1995**, *187*, 351–365. [[CrossRef](#)]
47. Ouyang, Y.; Zheng, C. Surficial processes and CO₂ flux in soil ecosystem. *J. Hydrol.* **2000**, *234*, 54–70. [[CrossRef](#)]
48. Horton, R.; Aguirre-Luna, O.; Wierenga, P.J. Observed and predicted two-dimensional soil temperature distributions under a row crop. *Soil Sci. Soc. Am. J.* **1984**, *48*, 1147–1152. [[CrossRef](#)]
49. Pangle, R.E.; Seiler, J. Influence of seedling roots environmental factors and soil characteristics on soil CO₂ efflux rates in a 2-year-old loblolly pine (*Pinus taeda* L.) plantation on the virginia piedmont. *Environ. Pollut.* **2002**, *116*, S85–S96. [[CrossRef](#)]
50. Epron, D.; Nouvellon, Y.; Rouspard, O.; Mouvondy, W.; Mabilab, A.; Laurent, S.A.; Joffre, R.; Jourdan, C.; Bonnefond, J.M.; Berbigier, P.; et al. Spatial and temporal variations of soil respiration in a *Eucalyptus* plantation in Congo. *For. Ecol. Manag.* **2004**, *202*, 149–160. [[CrossRef](#)]
51. Han, G.; Zhou, G.; Xu, Z.; Yang, Y.; Liu, J.; Shi, K. Biotic and abiotic factors controlling the spatial and temporal variation of soil respiration in an agricultural ecosystem. *Soil Biol. Biochem.* **2007**, *39*, 418–425. [[CrossRef](#)]
52. Maestre, F.T.; Cortina, J. Small-scale spatial variation in soil CO₂ efflux in a mediterranean semiarid steppe. *Appl. Soil Ecol.* **2003**, *23*, 199–209. [[CrossRef](#)]

